RF CONDITIONING AND MICROWAVE GUN SIMULATIONS FOR THE UNIVERSITY OF HAWAI'I LINAC AND FEL

N. Bidault*, S. Li
University of Hawai'i at Mānoa, Honolulu, HI, USA

Abstract

The S-band electron linac and free-electron-laser facility at the University of Hawai'i at Mānoa is being recommissioned after an extended period of inactivity. Following the restoration of vacuum and thermionic cathode systems, recent work focused on the high-power RF chain and on conditioning of the linac and microwave electron gun. We report RF conditioning measurements obtained during progressive power-up sessions at 1–4 Hz, including forward power delivered to the linac and forward and reflected power at the microwave gun. The linac RF response is stable and consistent with legacy calibrations, while the gun exhibits strong multipacting signatures. To guide the next conditioning campaign, we also present the developing RF-Track model of the thermionic TM_{010} gun, incorporating field maps, space charge, and beam loading.

INTRODUCTION

The University of Hawai'i Free Electron Laser (UH FEL) facility is based on a compact S-band injector and traveling-wave linac originally developed as part of the Mark-III/Mark-V FEL program. The accelerator produces electron beams for a mid-infrared FEL oscillator and for inverse Compton scattering x-ray experiments [1]. The previous recommissioning activities included the restoration of the vacuum, the installation of a thermionic cathode, and the upgrade of a low-level RF preamplifier, after the facility had remained inactive for several years [2]. The present paper reports the next step in that effort: reconditioning the RF systems for beam operation and improving the injector model used to prepare for and interpret the next runs. The injector consists of a LaB_6 thermionic cathode installed in a single-cell 2856 MHz microwave gun operating in a TM_{010}-like mode. The gun is followed by an Enge alpha-magnet that serves as a compressor and momentum filter before the beam is injected into a 10-ft SLAC-type traveling-wave linac, which typically accelerates the beam to 35–45 MeV. The same high-power klystron chain feeds the linac and the microwave gun through separate RF distribution branches. The RF conditioning, therefore, provides information not only on the available linac accelerating power, but also on the state of the gun cavity and its waveguide section, which are critical for stable beam emission and injection.

RF SYSTEM UPGRADES

The renewed low-level RF (LLRF) system was designed to provide a clean and reproducible S-band drive for the klystron. The 2856 MHz drive is generated by a new signal generator locked to a 10 MHz reference via a GPS disciplined oscillator. A frequency counter measures the quality of the generated signal, using an independent 10 MHz reference from a rubidium frequency standard. The timing signal generation was also upgraded to support reproducible pulsed operation during RF conditioning. The RF drive chain includes a new solid-state preamplifier that drives the high-power klystron. Stand-alone tests of the preamplifier showed an output power of approximately 58.4 dBm (about 700 W), with a measured pulse stability of 5×10^{-3} dBm and rise and fall times of about 11 ns. These measurements provide a baseline for the reproducibility expected from the LLRF and driver chain. High-voltage conditioning of the pulse-forming network and thyratron modulator was completed before RF conditioning, and the klystron perveance was measured near the nominal value of 1.7 μA $V^{-3/2}$ at 36.5 kV.

RF CONDITIONING RESULTS

RF conditioning was performed in several sessions, each lasting a few hours. The procedure consisted of progressive increases of RF pulse duration, input drive, and repetition rate, with operation between 1 and 4 Hz. The klystron and modulator behaved as expected throughout the conditioning runs, with no indication of sparking of abnormal high-voltage behavior during the power scans. Before increasing the RF power in the gun branch, frequency scans were performed to determine the microwave gun's effective resonant frequency at the current cooling-water temperature. The cavity response indicated a resonance at $f = 2859.85$ MHz. The RF drive was then increased progressively while recording the linac forward power (P_{LFP}) and gun forward power (P_{GFP}). The signals were acquired in the control room with a 6 GHz oscilloscope after propagation through the attenuation chains connected to the linac and gun RF couplers. Although the measured control-room signals are only at the level of a few dBm, Fig. 1 reports the inferred powers delivered to the linac and gun after applying the corresponding calibration and attenuation factors.

The measurements were performed at 1 Hz and repeated across several data sets to quantify shot-to-shot stability. The power levels are close to the historical operating regime, with P_{GFP} near 1 MW and P_{LFP} near 33 MW [3]. Figure 1 shows three input-power settings, corresponding to 0, +1, and +2 dBm from the 2856 MHz signal generator before amplification by the klystron driver. The linac forward power increases consistently with the applied RF drive and remains comparatively stable over the pulse. This behavior confirms

* nbidault@hawaii.edu

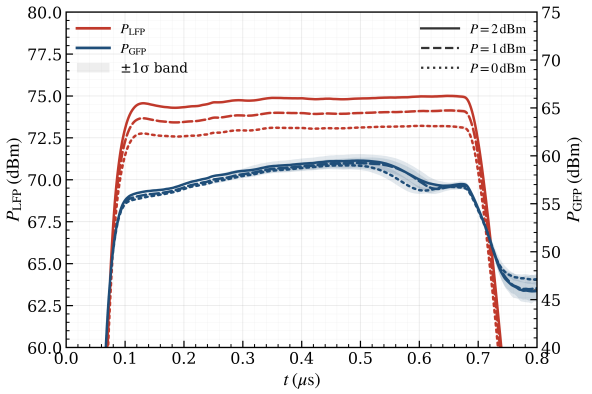

Figure 1: Shot-to-shot RF-conditioning measurements for the linac and microwave-gun forward powers. The shaded regions indicate the measured one-standard-deviation pulse-to-pulse variation.

that the preamplifier, klystron, modulator, RF distribution, and linac branch are operating close to the expected conditioning point. The microwave gun branch shows a different response. The gun forward power does not increase proportionally with the RF drive and exhibits sharp pulse-to-pulse instabilities, visible as a large one-standard-deviation band around the average curves. In parallel, pressure rises were observed in the microwave-gun vacuum sector. We therefore attribute the observed RF instabilities to multipactoring in the gun cavity or in the nearby waveguide section. The present measurements indicate that the cavity and gun sector still require additional RF processing. The conditioning campaign was paused to avoid continuing high-power operation without the first beam diagnostic downstream of the gun. This diagnostic, a thin toroidal current transformer located before the alpha magnet, is presently compromised and is being prepared for repair or replacement. Resuming RF conditioning with a working current monitor will allow the next campaign to correlate RF signatures with emitted electron charges.

MICROWAVE GUN MODEL

The RF conditioning results motivate a more detailed model of the injector. The goal is to connect the observed gun RF behavior to the beam parameters expected at the gun exit and to provide reliable input distributions for the alpha magnet, linac, diagnostic chicane, and FEL simulations. The model uses field maps generated with Remcom XFdtd, a three-dimensional finite-difference time-domain solver based on a Yee-cell grid. The fields are transformed into the RF-Track (Refs. [4] and [5]) coordinate system and used for particle tracking in the TM_{010} cavity, as shown in the bottom plot of Fig. 2.

The model reconstructs the RF phasor from two field-map snapshots separated by approximately 90 degrees in RF phase. Short phase scans are first used to verify the accelerating phase and estimate the effective voltage and R/Q for the beam-loading model.

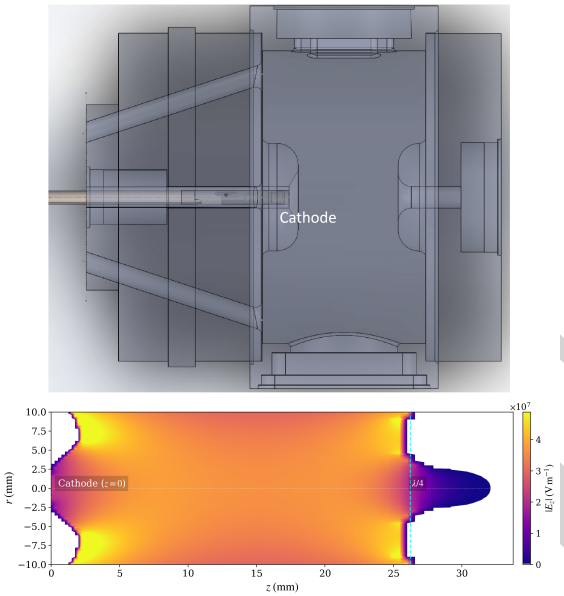

Figure 2: Microwave-gun model used for RF-Track simulations: cavity geometry with the inserted cathode and axial electric-field map from the 3-D FDTD solver.

$$J = A_R T^2 \exp\left[-\frac{1}{k_B T}\left(\phi - \sqrt{\frac{e^3 E}{4\pi\varepsilon_0}}\right)\right]. \qquad (1)$$

Thermionic emission is modeled using a time-dependent Richardson–Dushman model that includes Schottky lowering at the cathode surface, as in Eq. (1). Here J is the emitted current density normal to the cathode surface, A_R is the Richardson constant, T is the cathode temperature, k_B is the Boltzmann constant, ϕ is the effective work function of the LaB_6 emitting surface, e is the elementary charge, ε_0 is the vacuum permittivity, and E is the instantaneous surface electric field. The square-root term represents the RF-field-induced reduction of the emission barrier. Since E varies during the S-band cycle, the source current is naturally phase-gated.

In the tracking model, Eq. (1) is evaluated using the on-axis field extracted at the cathode plane. The transverse coordinates are sampled on the emitting disk, the transverse momenta include thermal spread and an optional cathode-surface roughness contribution, and the longitudinal momentum follows a Maxwell-Boltzmann flux distribution. The nominal studies use a cathode temperature of 1650 K, an effective work function of 2.1 eV, and 10^5 macroparticles. Figure 3 summarizes the present source and tracking diagnostics. The emission-time spectrum follows the analytical current-density profile given by Eq. (1); particles are tagged as either transmitted through the cavity or going backward. The transverse and longitudinal Twiss-parameter evolution through the cavity provides a compact description of the beam accepted by the downstream alpha magnet. In particular, the rapid variation of the Twiss functions in the first centimeters of tracking reflects the low-energy regime in which

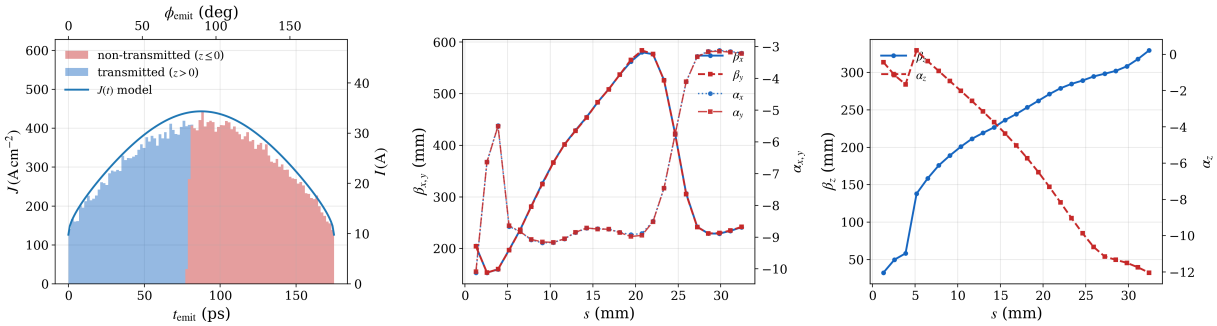

Figure 3: Emission model and simulated beam evolution in the microwave gun: emission-time spectrum, transverse Twiss parameters, and longitudinal Twiss parameters.

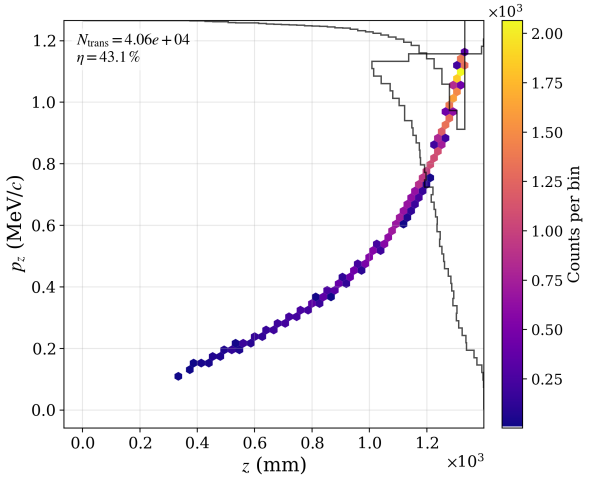

Figure 4: Longitudinal phase space of the transmitted beam at the gun exit, with projections on the z and p_z axes.

acceleration, focusing, and collective effects are strongly coupled. The longitudinal phase space at the exit of the cavity is shown in Fig. 4. The distribution retains the correlation imposed by emission over a finite RF phase interval and by acceleration in the standing-wave field. This output distribution is the relevant input for subsequent studies of the alpha-magnet momentum filter. Space charge and beam loading are included because both effects can influence capture in the low-energy part of the gun. Both effects are also strongly dependent on the electron beam charge density, which is controlled by the cathode temperature. For this study, the cathode temperature is modest (1650 K). The RF-Track space-charge solver is applied during emission and transport; typical studies use a space-charge kick step of 0.1 mm/c and 200 kicks over the emission window. Beam loading is treated with a standing-wave cavity model using $Q_0 \simeq 4000$, $Q_{ext} \simeq 3500$, one effective cell, and a loaded quality factor derived from these values. The collective-effects step is typically 0.1 mm/c. The present version of the model is already used to study transmission through the cavity, the final longitudinal momentum distribution of transmitted electrons, and the evolution of the Twiss parameters through the gun. The code used for these studies is available in Ref. [6]. The model will be connected to existing injector and transport simulations so that the microwave gun output feeds the alpha-magnet momentum filter, the linac, the diagnostic chicane, and ultimately, the FEL undulator. The optimization algorithms developed in the parallel FELsim study, including gradient-based and Bayesian approaches for beam matching, provide the first step toward model-based tuning of this complete framework [7].

CONCLUSION

The RF recommissioning of the UH accelerator has progressed from LLRF and high-voltage recovery to high-power conditioning of the linac and microwave gun. The upgraded preamplifier, klystron, and modulator behaved as expected during the recent conditioning runs. Progressive RF-drive scans showed that the linac forward power reaches the expected operating range and scales consistently with the input drive. The microwave gun branch shows stronger limitations and exhibits large shot-to-shot instabilities, accompanied by pressure rises in the gun vacuum sector. In parallel, a detailed RF-Track model of the thermionic TM_{010} microwave gun is being developed. This model will be incorporated into the existing start-to-end framework for the alpha magnet, linac, diagnostic chicane, and FEL undulator. Ongoing work includes generating additional field map sets to analyze transient cavity turn-on, studying residual gas ionization, and using beam measurements to constrain the model as operations resume.

ACKNOWLEDGEMENTS

This work is supported by start-up funds provided by the University of Hawai‘i at Mānoa to N. Bidault, and by the U.S. Department of Energy, Office of Science, Office of Basic Energy Sciences, under Contract No. DE-SC0025583.

REFERENCES

[1] P. Niknejadi *et al.*, “Free-electron laser inverse-Compton interaction X-ray source”, *Phys. Rev. Accel. Beams*, vol. 22, no. 4, p. 040704, 2019. doi:10.1103/PhysRevAccelBeams.22.040704

[2] N. Bidault, S. Li, H. Puwar, and A. Weinberg, “Recommissioning of the University of Hawai’i LINAC and Free Electron Laser”, in *Proc. IPAC’25*, Taipei, Taiwan, Jun. 2025, pp. 1175–1178. doi:10.18429/JACoW-IPAC2025-TUPM005

[3] M. Hadmack *et al.*, "Electron bunch energy and phase feedforward stabilization system for the Mark V RF-linac free-electron laser", *Rev. Sci. Instrum.*, vol. 84, p. 063302, 2013. doi:10.1063/1.4809938

[4] A. Latina, "RF-Track: Beam tracking in field maps including space-charge effects, features and benchmarks", in *Proc. LINAC'16*, East Lansing, MI, USA, Sep. 2016, pp. 104–107. doi:10.18429/JACoW-LINAC2016-MOPRC016

[5] A. Latina, *RF-Track*, CERN GitLab repository. https://gitlab.cern.ch/rf-track

[6] N. Bidault, *RF-TRACK UH Thermionic RF Gun*, GitHub repository. https://github.com/Ioniels/RF-TRACK_UH_ThermionicRFgun

[7] N. Bidault, S. H. P. Chan, C. Komo, S. Li, and E. Valetov, "Deterministic methods and Bayesian optimization algorithms applied to the UH Manoa Linac", presented at IPAC'26, Deauville, France, May 2026, paper MOP6318, this conference.